

Characterization of Complex Industrial Specimens by Hyperspectral EPMA Mapping

Aaron Torpy¹, Nicholas C. Wilson¹, and Colin M. MacRae¹

¹ Microbeam Lab, CSIRO Mineral Resources, Private Bag 10, Clayton South, VIC, 3169, Australia.

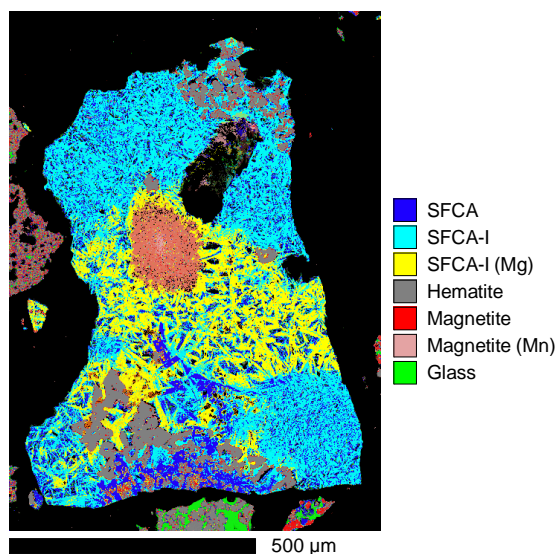
The characterization of mineral or metallurgical specimens from industry can present a number of significant challenges. Often, geological or mineral processing specimens contain both many elements (>10) and many mineral phases (>10), some of which may differ in composition in small yet critical degrees. Both metallurgical and mineral systems can exhibit significant solid solution chemistry, meaning that phases do not have discrete or well-defined compositions. Furthermore, mineral and mineral processing specimens display compositional or morphological heterogeneity over length scales from the sub-micron (e.g. nano-precipitation / intergrowths) to the macroscopic (e.g. metasomatism), requiring techniques that can rapidly characterize large specimens at fine spatial resolution. Moreover, the opportunity to characterize industrial problems typically only arise when a process has unexpectedly failed, such as may occur with the presence of unexpected elements and/or unexpected phases, requiring the problems to be solved with little (or sometimes incorrect) *a priori* knowledge. In such instances, the urgency of the problem may also be great, requiring the problems to be solved efficiently with short turnaround times, and without the ability to reproduce the faulty process under controlled conditions.

The modern electron probe micro-analyser (EPMA) is particularly well suited to solve these complex industrial problems. Equipped with as many as five wavelength dispersive spectrometers (WDS), as well as one or more silicon drift energy dispersive detectors (SDD EDS), the EPMA excels at precise quantification of elemental compositions with trace sensitivity (10s of ppm). The recent development of soft-x-ray emission spectroscopy detectors (SXES) for use with EPMA has further extended the applicability of the EPMA to spectrometry of lithium, as well as chemical state spectroscopy using L, M and N x-ray lines [1]. In addition to x-rays, the integrated light optics in an EPMA allows the efficient collection of cathodoluminescence, which may reveal subtle chemical or structural variations not readily detectable by x-rays, such as ppm-level zonation of trace dopants [2], or radiation-induced metamictization [3]. Critically, all these signals may be collected simultaneously in a single-pass EPMA beam or stage map [4], which permits high-throughput characterisation of large areas without detailed *a priori* knowledge. Furthermore, the advent of field emission gun equipped EPMA has brought greater beam currents into smaller spot sizes at lower accelerating voltages, allowing greater chemical sensitivity at finer length scales.

Routine hyperspectral mapping in a highly automated EPMA presents some challenges for data interpretation. An EPMA may produce of the order of 100GB of data (uncompressed) in a 24 hour period, and may run essentially non-stop for weeks, excluding brief pauses for sample changes. For the data analyst to keep pace with this acquisition rate within a mere 7.35 hour workday, an efficient data reduction strategy is required to extract the critical information to solve the industrial problem. It is also essential that the data reduction process operates without *a priori* knowledge of which elements, phases or variations are likely to be present, and does not conceal or discard unexpected results.

Our laboratory operates two FEG-EPMA (JEOL JXA8500F, and JXA 8530F [5]), which are both equipped for simultaneous WDS and hyperspectral EDS and CL mapping. Following acquisition, map data is first partitioned into clusters of statistically indistinguishable pixels using a 3-sigma window

based on their WDS and EDS x-ray intensities using the in-house developed CHIMAGE software [6]. Following partitioning, the clusters are sorted into a hierarchical tree based on compositional similarity. This clustering regime reduces the circa 1 million pixels from a typical map into approximately 5,000 clusters of statistically distinct compositions. Nearest neighbour analysis of the spatial distribution of clusters sifts the clusters into those that were present as spatially integral regions of consistent composition ('phases'), and excluded clusters due to solid solutions, edge effects, or sub-pixel mixing. The EDS spectrum of each cluster is then integrated from the hyperspectral map, and quantified using top-hat filtered linear least squares regression against spectra of known standards, coupled with matrix correction using the XPP algorithm as implemented in the STRATAGEM library [7]. Following quantification, the identity of the clusters due to solid solutions, edge effects and sub-pixel mixing are determined by linear least-squares deconvolution of the k-ratios each cluster against the k-ratios of the 'end member' phases identified by quantification. The result of this process is a phase map identifying the phase(s) of each pixel (e.g. Figure 1, showing phases in a sintered iron ore [8]), plus the spectra and quantitative compositions for each corresponding phase (e.g. table 1). The phase solution may be applied to subsequent maps in a series, allowing high throughput analysis and consistent representation of results. However, if unexpected phases in subsequent maps do not match the pre-defined phase identifications (within 3-sigma), these clusters may be readily highlighted, their composition quantified and their identification determined, all in the period of a few seconds to a few minutes.



Phase	Fe	Ca	Mg	Mn	Al	Si	O	Total
SFCA	50.0	9.9	0.4	0.2	1.9	3.3	31.4	97.4
SFCA-I	54.6	9.1	0.5	0.4	1.3	1.3	30.2	97.4
SFCA-I (Mg)	56.9	6.5	1.5	0.7	1.1	0.9	30.3	98.1
Hematite	67.1	0.2	0.0	0.1	0.5	0.1	29.6	97.9
Magnetite	66.0	1.1	1.0	0.4	0.6	0.1	27.1	96.5
Glass	11.3	25.5	0.3	0.1	2.5	17.9	38.2	96.6

Table 1. (above) Compositions of iron ore sinter phases measured by quantitative analysis of clustered EDS spectra, in weight percent. Analysed elements with concentrations below detection limits for all phases have been excluded from the table.

Figure 1. (left) Clustered phase map of a sinter grain, showing hematite and magnetite bonded by several distinct silico-ferrites of calcium and aluminium (SFCA, SFCA-I and SFCA-I (Mg)).

References:

- [1] H Takahashi *et al.*, IOP Conference Series: Materials Science and Engineering **109** (2016)
- [2] WP Leeman *et al.*, Microscopy and Microanalysis **18**, No. 6, (2012) p. 1322-1241.
- [3] CM MacRae *et al.*, Microscopy and Microanalysis **18** Suppl. 2, (2012) p. 1002-1003.
- [4] CM MacRae, *et al.*, Proceedings of AMAS VI (2001), Sydney, Australia, p. 68-69.
- [5] We acknowledge support from ARC – LE130100087
- [6] CM MacRae, *et al.*, Microscopy Research and Technique **67** (2005) p. 271-277.
- [7] J L Pouchou, Analytica Chimica Acta **283** (1993) p. 81-97.
- [8] A Torpy, *et al.*, Proceedings of AMAS XIV, 6-10 Feb., 2017, Brisbane, Australia, p. 102-103.